JOC Article

Regioisomerically Controlled Self-Aggregation of Zinc 3-Hydroxymethyl-13-formyl-chlorin/Porphyrin and Their 3,13-Inverted Pigments

Michio Kunieda and Hitoshi Tamiaki*

Department of Bioscience and Biotechnology, Faculty of Science and Engineering, Ritsumeikan University, Kusatsu, Shiga 525-8577, Japan

tamiaki@se.ritsumei.ac.jp

Received November 13, 2006

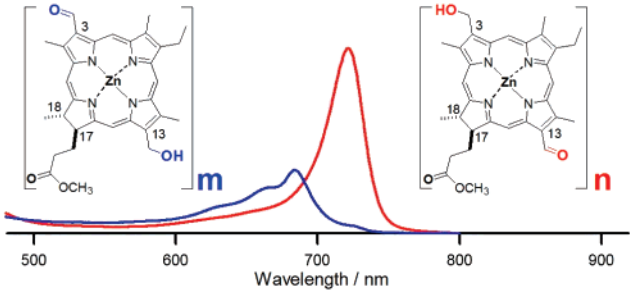

Zinc 3-hydroxymethyl-13-formyl-chlorin, **1**, and its 3,13-inverted (3-formyl-13-hydroxymethyl) regioisomer, **2**, and their corresponding 17,18-dehydrogenated porphyrins, **3** and **4**, were synthesized for models of natural bacteriochlorophylls-*c*/*d*/*e* possessing 3^1-OH and 13-C═O groups which self-aggregate in main light-harvesting antenna systems of green photosynthetic bacteria. Zinc chlorins **1** and **2** were monomers in neat THF and gave an obvious difference in their visible absorption spectra, indicating that sole inversion of the 3- and 13-substituents in a chlorin chromophore controlled their optical properties. In an aqueous Triton X-100 solution (a nonionic surfactant), zinc 3^1-OH-13-CHO-chlorin **1** and porphyrin **3** self-aggregated as do natural bacteriochlorophylls, while zinc 3-CHO-13^1-OH chlorin **2** and porphyrin **4** (the 3,13-inverted regioisomers of **1** and **3**) hardly formed such large oligomers, showing that the inversion of the peripheral 3,13-substituents made their oligomerization unfavorable. FT-IR spectra of aggregated **1**−**4** in the solid film and their molecular modeling calculations suggested that the 17^2-C═O moiety in inverted **2**/**4** interacted with its own 13^1-OH group to disturb further aggregation.

Introduction

Green photosynthetic bacteria have unique light-harvesting antenna systems (chlorosomes), in which numerous bacteriochlorophyll(BChl)-*c*/*d*/*e* molecules possessing 3^1-OH, Mg, and 13-C═O moieties (see Figure 1, upper) self-aggregate by using their specific intermolecular interactions, as in coordination (3^1-O···Mg) and hydrogen bonding (3^1-OH···O═C-13).[1] In a chlorosome, many BChl molecules excitonically couple to form large oligomers and harvest sunlight energy, and the energy then migrates without significant loss. The isolated chlorosomal BChls easily self-aggregate in both nonpolar organic and aqueous micellar solutions to form similar large oligomers.[2] Such facile self-aggregation has attracted a great deal of attention for the development of various applications including artificial light-harvesting systems and photoactive nanodevices.

* To whom correspondence should be addressed. Phone: (+81)77-566-1111. Fax: (+81)77-561-2659.

(1) (a) Blankenship, R. E.; Matsuura, K. In *Light Harvesting Antennas in Photosynthesis*; Green, B. R., Parson, W. W., Eds.; Kluwer Academic Publisher: Dordrecht, The Netherlands, 2003; pp 195−217. (b) Tamiaki, H. *Photochem. Photobiol. Sci.* **2005**, *4*, 675−680. (c) Miyatake, T.; Tamiaki, H. *J. Photochem. Photobiol., C* **2005**, *6*, 89−107.

(2) (a) Smith, K. M.; Kehres, L. A.; Fajer, J. *J. Am. Chem. Soc.* **1983**, *105*, 1387−1389. (b) Brune, D. C.; Nozawa, T.; Blankenship, R. E. *Biochemistry* **1987**, *26*, 8644−8652. (c) Holzwarth, A. R.; Griebenow, K.; Schaffner, K. *J. Photochem. Photobiol., A* **1992**, *65*, 61−71. (d) Uehara, K.; Olson, J. M. *Photosynth. Res.* **1992**, *33*, 251−257. (e) Hirota, M.; Moriyama, T.; Shimada, K.; Miller, M.; Olson, J. M.; Matsuura, K. *Biochim. Biophys. Acta* **1992**, *1099*, 271−274. (f) Tamiaki, H. *Coord. Chem. Rev.* **1996**, *148*, 183−197. (g) Saga, Y.; Matsuura, K.; Tamiaki, H. *Photochem. Photobiol.* **2001**, *74*, 72−80. (h) Mizoguchi, T.; Saga, Y.; Tamiaki, H. *Photochem. Photobiol. Sci.* **2002**, *1*, 780−787. (i) Saga, Y.; Akai, S.; Miyatake, T.; Tamiaki, H. *Bioconjugate Chem.* **2006**, *17*, 988−994.

10.1021/jo0623282 CCC: $37.00
Published on Web 03/06/2007

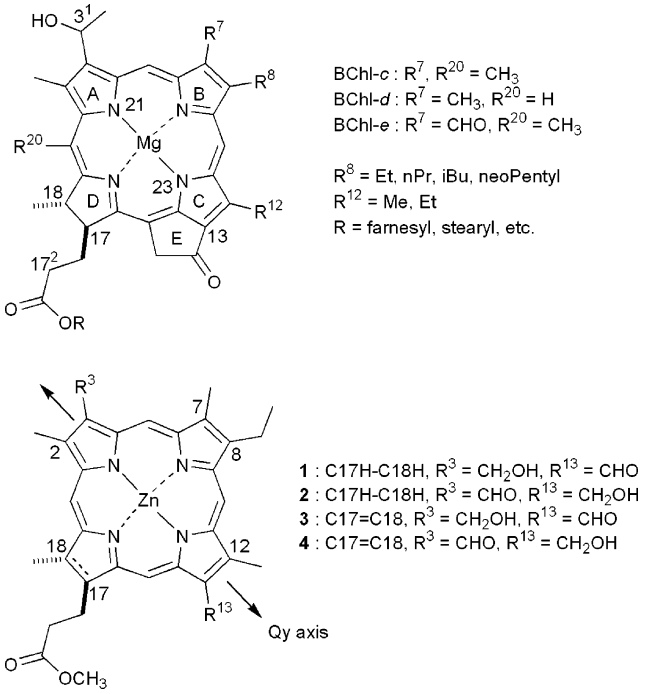

FIGURE 1. Molecular structures of natural BChls-*c*/*d*/*e* (upper), synthetic zinc chlorins **1**/**2**, and porphyrins **3**/**4** possessing 3-/13-hydroxymethyl and 13-/3-formyl groups (lower). An arrow drawn in the lower structure indicates the Qy axis, a transition dipole moment of a chlorin chromophore.

Many synthetic model compounds possessing the above structural motif have been reported and self-aggregated similarly to the above natural BChls.[1c,3] Structural requirements for the chlorosomal self-aggregation have been partially clarified as follows: (i) π-conjugate systems (porphyrin,[3f,j,4] chlorin,[3a,c,5] and bacteriochlorin[6]) and (ii) the interactive moieties (OH, coordinative metal, and C═O) in a line.[3f,7] Elucidation of such requisite elements would be of great advantage for constructing efficient light-harvesting antenna models.

On the basis of the molecular structure of BChl-*c*, those of BChls-*d* and -*e* are 20-demethylated and 7-formylated, respectively (see upper drawing of Figure 1).[8] Some alkyl groups including methyl, ethyl, propyl, isobutyl, and neopentyl groups are found at the 8,12-positions, and various long hydrocarbon chains are esterified at the 17^2-position.[9] These alterations which might be dependent on the living conditions of bacteria affect the optical properties of the BChl self-aggregates but never suppress intermolecular interactions (coordination and hydrogen bonding) in their self-aggregation. Slight modifications of the interactive moieties (primary, secondary, and tertiary 3^1-OH;[3b] Mg, Zn, and Cd as the central metal;[3d] fixed and flexible 13-C═O including aldehyde, keto, and ester functions[3f,10]) are acceptable for the chlorosomal self-aggregation. Here we report the synthesis and self-aggregation of zinc 3-hydroxymethyl-13-formyl-chlorin **1** and its 3,13-inverted regioisomer **2** by modification of naturally occurring chlorophyll(Chl)-*a* and also those of their corresponding 17,18-dehydrogenated porphyrins **3** and **4** (see lower drawing of Figure 1).

Results and Discussion

Synthesis of Zinc Chlorins 1/2 and Porphyrins 3/4 by Modifying Naturally Occurring Chl-*a*. Zinc chlorins and porphyrins **1**−**4** were synthesized from rhodochlorin XV dimethyl ester (**5**)[11] prepared by modifying Chl-*a* (Scheme 1). Both the 13- and 17^2-methoxycarbonyl groups in **5** were reduced by LAH to give the diol **6** in 92% yield. The resulting primary alcoholic moieties in **6** were simultaneously oxidized by combination of tetrapropylammonium perruthenate with *N*-methylmorpholine *N*-oxide, affording the corresponding 13,-17^2-diformyl-chlorin **7** (42%). The more reactive 17^2-formyl group in **7** (due to its unconjugation with a chlorin π-system) was selectively oxidized to the carboxy group and successively esterified by ethereal diazomethane to give 13-formyl-17^2-methoxycarbonyl-chlorin **8** (67%). Oxidative cleavage of the 3-vinyl group in **8** by catalytic OsO_4 with aqueous $NaIO_4$ gave 3,13-diformyl-17^2-methoxycarbonyl-chlorin **9** (66%). After zinc insertion to **9**, the sole 3- or 13-formyl group in **10** was carefully reduced, affording a regioisomeric mixture of zinc chlorins **1** and **2** possessing hydroxymethyl and formyl groups at the 3- or 13-position and a small amount of undesired doubly reduced diol **11** after FCC separation.

Separation of regioisomeric **1** (normal-type, like natural chlorosomal BChls) with its inverted-**2** was easily achieved by usual reverse-phase HPLC (methanol/water/pyridine = 90/9/1). The HPLC chromatogram of the mixture showed two main elutions: the first (f1) and second (f2) fractions eluted at 13 and 15 min, respectively. The molecular structures of the separated pigments were confirmed by intramolecular $^1H-^1H$ correlations on their NOESY spectra (see Figure 2). Starting from the easily assigned 18-CH_3, 15-H, 20-H, and 2-CH_3 were determined. The NOE spectrum of f1 showed obvious correlations between the 2-CH_3 (3.33 ppm) and a 2H singlet (5.84 ppm) and between the 15-H (9.33 ppm) and 1H singlet

(3) (a) Tamiaki, H.; Amakawa, M.; Shimono, Y.; Tanikaga, R.; Holzwarth, A. R.; Schaffner, K. *Photochem. Photobiol.* **1996**, *63*, 92−99. (b) Yagai, S.; Miyatake, T.; Shimono, Y.; Tamiaki, H. *Photochem. Photobiol.* **2001**, *73*, 153−163. (c) Yagai, S.; Tamiaki, H. *J. Chem. Soc., Perkin Trans. 1* **2001**, 3135−3144. (d) Tamiaki, H.; Amakawa, M.; Holzwarth, A. R.; Schaffner, K. *Photosynth. Res.* **2002**, *71*, 59−67. (e) Tamiaki, H.; Omoda, M.; Saga, Y.; Morishita, H. *Tetrahedron* **2003**, *59*, 4337−4350. (f) Tamiaki, H.; Kimura, S.; Kimura, T. *Tetrahedron* **2003**, *59*, 7423−7435. (g) Balaban, T. S.; Bhise, A. D.; Fischer, M.; Linke-Schaetzel, M.; Roussel, C.; Vanthuyne, N. *Angew. Chem., Int. Ed.* **2003**, *42*, 2140−2144. (h) Sasaki, S.; Tamiaki, H. *Bull. Chem. Soc. Jpn.* **2004**, *77*, 797−800. (i) Balaban, T. S.; Tamiaki, H.; Holzwarth, A. R. In *Supramolecular Dye Chemistry*; Würthner, F., Ed.; Topics in Current Chemistry, Vol. 258; Springer: Heidelberg, Germany, 2005; pp 1−38. (j) Tamiaki, H.; Kitamoto, H.; Watanabe, T.; Shibata, R. *Photochem. Photobiol.* **2005**, *81*, 170−176. (k) Balaban, T. S. *Acc. Chem. Res.* **2005**, *38*, 612−623. (l) Mizoguchi, T.; Shoji, A.; Kunieda, M.; Miyashita, H.; Tsuchiya, T.; Mimuro, M.; Tamiaki, H. *Photochem. Photobiol. Sci.* **2006**, *5*, 291−299.

(4) Balaban, T. S.; Linke-Schaetzel, M.; Bhise, A. D.; Vanthuyne, N.; Roussel, C. *Eur. J. Org. Chem.* **2004**, 3919−3930.

(5) (a) Sasaki, S.; Omoda, M.; Tamiaki, H. *J. Photochem. Photobiol., A* **2004**, *162*, 307−315. (b) Huber, V.; Katterle, M.; Lysetska, M.; Würthner, F. *Angew. Chem., Int. Ed.* **2005**, *44*, 3147−3151.

(6) (a) Kunieda, M.; Mizoguchi, T.; Tamiaki, H. *Photochem. Photobiol.* **2004**, *79*, 55−61. (b) Kunieda, M.; Tamiaki, H. *J. Org. Chem.* **2005**, *70*, 820−828.

(7) (a) Jesorka, A.; Balaban, T. S.; Holzwarth, A. R.; Schaffner, K. *Angew. Chem., Int. Ed.* **1996**, *35*, 2861−2863. (b) Yagai, S.; Miyatake, T.; Tamiaki, H. *J. Photochem. Photobiol., B* **1999**, *52*, 74−85. (c) Yagai, S.; Miyatake, T.; Tamiaki, H. *J. Org. Chem.* **2002**, *67*, 49−58.

(8) Scheer, H. In *Light Harvesting Antennas in Photosynthesis*; Green, B. R., Parson, W. W., Eds.; Kluwer Academic Publisher: Dordrecht, The Netherlands, 2003; pp 29−81.

(9) Tamiaki, H.; Shibata, R.; Mizoguchi, T. *Photochem. Photobiol.* **2007**, *83*, 152−162.

(10) (a) Tamiaki, H.; Shimamura, Y.; Yoshimura, H.; Pandey, S. K.; Pandey, R. K. *Chem. Lett.* **2005**, *34*, 1344−1345. (b) Kunieda, M.; Tamiaki, H. *Eur. J. Org. Chem.* **2006**, 2352−2361.

(11) Smith, K. M.; Lewis, W. M. *Tetrahedron, Suppl.* **1981**, 399−403.

SCHEME 1. Synthesis of Zinc Chlorins and Porphyrins 1−4[a]

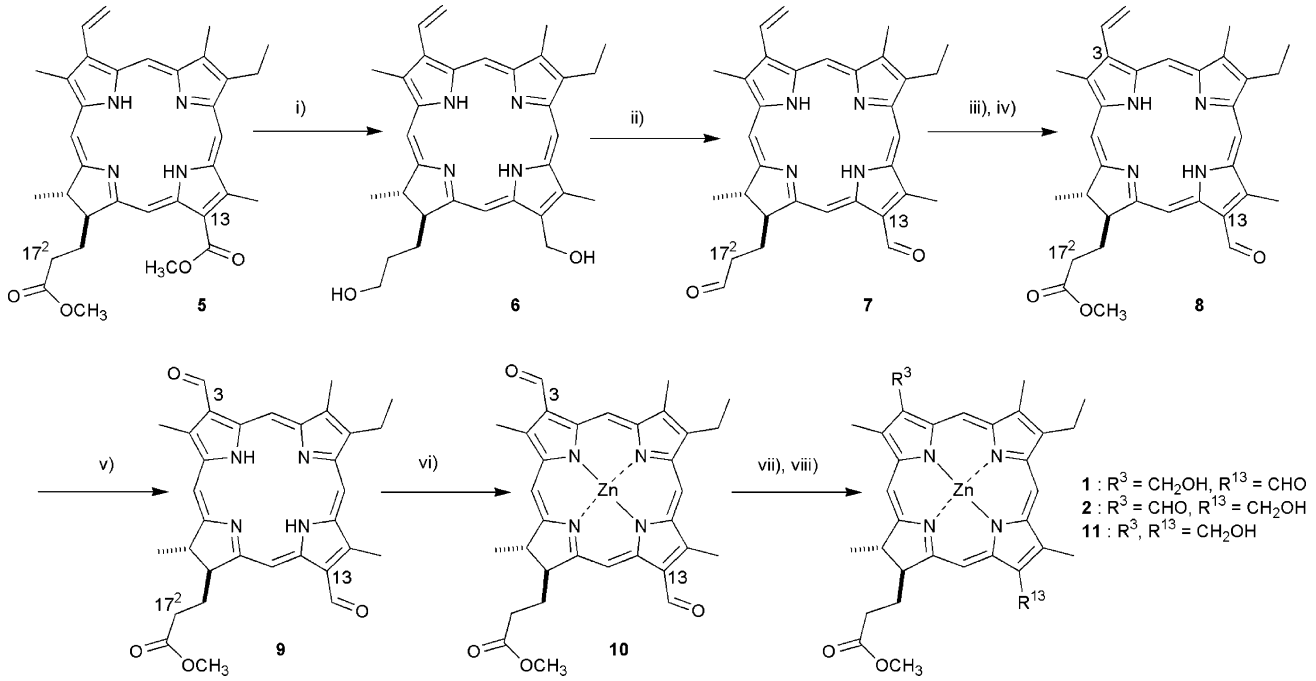

[a] Reagents and conditions: (i) LAH, THF; (ii) *N*-methylmorpholine *N*-oxide, *n*-Pr_4NRuO_4, CH_2Cl_2; (iii) $NaClO_2$, $HOSO_2NH_2$, THF−2-methyl-2-butene−H_2O; (iv) ethereal CH_2N_2; (v) catalyst OsO_4, $NaIO_4$, THF−1,4-dioxane−H_2O; (vi) $Zn(OAc)_2$, $CHCl_3$−methanol; (vii) *t*-$BuNH_2BH_3$, CH_2Cl_2; and (viii) HPLC separation.

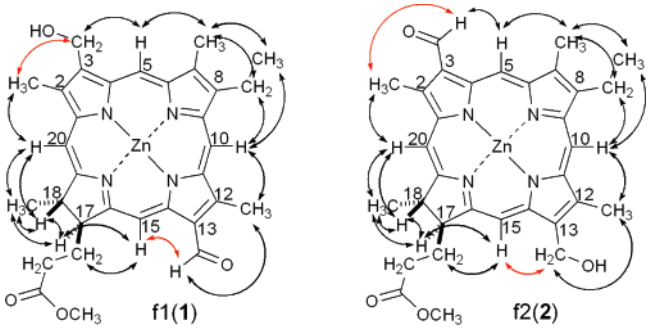

FIGURE 2. Observed $^1H-^1H$ NOE correlations of regioisomerically pure zinc chlorins **1** (left, f1) and **2** (right, f2). Important correlations are colored red.

(11.29 ppm), while that of f2 showed the correlations between the 2-CH_3 (3.71 ppm) and a 1H singlet (11.48 ppm) and between the 15-H (8.73 ppm) and 2H singlet (5.82 ppm). The specific 1H and 2H singlets at around 11 and 5.8 ppm were assigned to a formyl proton and hydroxymethyl protons, respectively. The NOE experiments clearly indicate that f1 was zinc 3[1]-OH-13-CHO-**1** and f2 was 3-CHO-13[1]-OH-**2**. The isolated yields for **1** and **2** were 42 and 13%, respectively, and little of the doubly reduced compound **11** was yielded, indicating that reduction of the 3-formyl group in **10** was more reactive than the 13-formyl group. The difference in the reduction could be due to a substituent effect in the chlorin π-system: the 3-position is farther from the reduced pyrrole ring than the 13-position.

17,18-Dehydrogenation of the regioisomerically pure **1** and **2** was carried out by DDQ,[12] affording the corresponding zinc porphyrins **3** or **4** in a quantitative yield.

(12) Tamiaki, H.; Watanabe, T.; Miyatake, T. *J. Porphyrins Phthalocyanines* **1999**, *3*, 45−52.

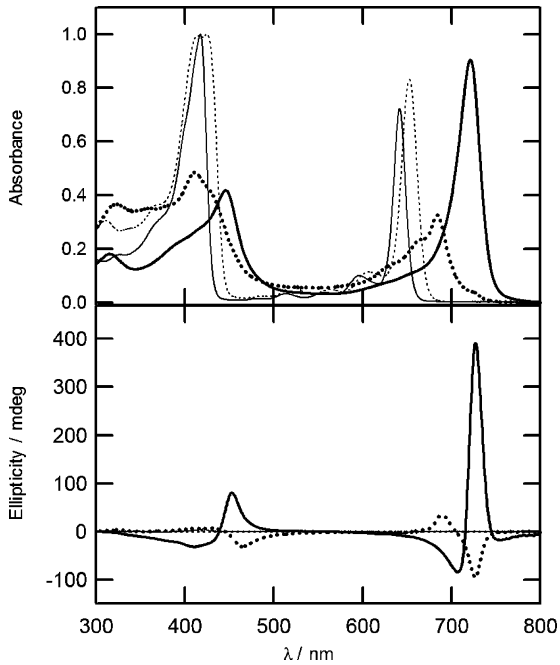

FIGURE 3. UV−vis (upper) and CD spectra (lower) of zinc chlorins **1** and its inverted-**2**. Thin solid/dotted lines were for **1**/**2** in THF, and bold solid/dotted lines were **1**/**2** in aqueous 0.0175 w/v % TX-100 solution containing 1.0 v/v % THF. Concentrations of all the samples were approximately 10 μM.

Optical Properties of Monomeric 1−4 in THF. THF solutions of zinc chlorins **1**/**2** showed sharp Qy absorption bands at around 600−680 nm with small CD signals (thin solid/dotted lines in Figure 3), indicating that a THF molecule is ligated to the central zinc atom of **1** or **2** to monomerize them and prevent any intermolecular interactions among their pigments, as shown

TABLE 1. UV−Vis Absorption Maxima of Zinc Complexes 1−4, 10, and 11 and Their Red-Shift Values (Δ) in Soret and Qy Bands by Their Self-Aggregation

	absorption maxima/nm[a]					
	Soret		Qy		Δ/cm^{-1}	
cmpd	monomer	aggregates	monomer	aggregates	Soret	Qy
1	418	446	642	722	1500	1730
2[b]	414	(412)	653	(660)		(160)
	425	436		684		700
				726		1540
3	423	485	601	647	3020	1180
4[b]	423	427	601	(605)		(110)
				631		790
10	437		676			
11	406		618			

[a] Monomers were observed in THF, and aggregates were observed in an aqueous 0.0175 w/v % TX-100 solution. Data in parentheses are ascribable to residual monomer peaks in the aqueous micellar solution. [b] Absorption maxima in the aqueous micellar solution were estimated from the second-derivative of the original spectra.

in natural BChls and their previous models.[3a] The UV−vis spectra of **1** and **2** were typical of a monomeric chlorin chromophore, and their Qy and Soret absorption maxima are situated between those of 3,13-CHO-**10** and 3^1,13^1-OH-**11** (Table 1). On the basis of **10** possessing two formyl groups at the 3- and 13-positions, reduction of one formyl group caused blue-shifts in both the Qy and Soret maxima (676/437 → 642/418 or 653/425 nm by **10** → **1** or **2**), and reductions of both caused further blue-shifts (676/437 → 618/406 nm by **10** → **11**). The relative intensities of the Qy absorption band to the Soret absorption (Abs) band (=Abs(Qy)/Abs(Soret)) decreased in the order of **10** (1.2) > **2** (0.83) ≈ **1** (0.72) > **11** (0.31). These are consistent with the previous reports;[7b,13] an electron-withdrawing substituent group on the Qy axis of a chlorin chromophore induces red-shifts in the Qy/Soret absorption bands with an enlargement of the Abs(Qy)/Abs(Soret) value. The Qy absorption maximum of inverted-**2** was situated at a longer wavelength than that of normal-**1**, and the Soret band in **2** was split. These spectral differences between normal-**1** and inverted-**2** were explained by the substituent effect of the 13- and 3-formyl groups as mentioned above. The present regioisomeric dependency is similar to the recent results reported by Lindsey and his colleagues:[13b] regioisomeric zinc chlorins possessing an electron-withdrawing TIPS-ethynyl group at the 3- or 13-position showed different UV−vis absorption maxima. The Qy absorption maxima of **1** and **2** in THF were simulated by the longest absorption peak positions estimated from ZINDO/S calculations,[6b] 643 and 661 nm for energetically minimized **1** and **2** ligated by a THF molecule (an axial ligand below the π-plane, α-ligand[14]).

In contrast to the different UV−vis spectra between zinc chlorins **1** and **2**, their corresponding 17,18-dehydrogenated porphyrins **3** and **4** did not show any differences in their UV−vis spectra in a THF solution (thin solid line in Figure 4, Table 1). Both the UV−vis spectra were typical of metalloporphyrin derivatives: a strong Soret band with less intense Q-bands. A fully conjugated metalloporphyrin π-system has a C_4 symmetry so that the substituent effect observed in a chlorin π-system was suppressed in the porphyrin π-system to give the same absorption properties in the regioisomers.

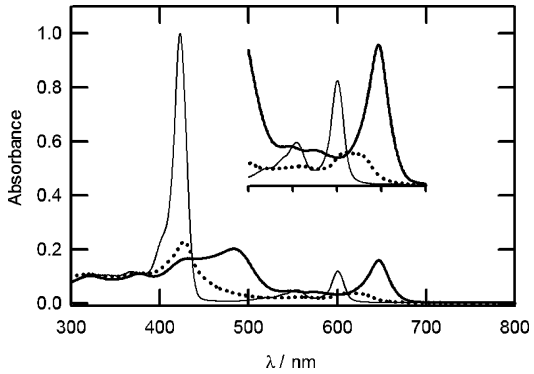

FIGURE 4. UV−vis spectra of zinc porphyrins **3** and its 3,13-inverted-**4**. The thin solid line was in THF solutions of **3** and **4** (both of which were identical), and bold solid/dotted lines were for **3**/**4** in aqueous 0.0250 w/v % TX-100 solution including 1.0 v/v % THF. Concentrations of all the samples were approximately 10 μM.

Self-Aggregation of Zinc Chlorins 1 and 2 in an Aqueous Triton X-100 (TX-100) Solution and a Solid Film. When a THF solution of **1** or **2** containing TX-100 (a nonionic surfactant) was diluted with a large amount of water (the final concentration of THF and TX-100 was 1.0 and 0.0175 w/v %, respectively), significant spectral changes were observed on both their UV−vis and CD spectra (see Figure 3 and Table 1). Zinc chlorin **1**, possessing the interactive groups in the natural order (3^1-OH/13-C=O), self-aggregated at the hydrophobic environment inside TX-100 micelles to form large oligomers as indicated by largely red-shifted Qy (642 → 722 nm) and Soret bands (418 → 446 nm) with strongly induced CD signals at around the region of newly appearing peaks (bold solid lines in Figure 3). These observations were clearly consistent with self-aggregation behaviors of natural BChls and their synthetic models. The red-shift value by self-aggregation of **1** was 1730 and 1500 cm^{-1} for Qy and Soret bands, respectively, which were comparable to those observed in similar chlorosomal self-aggregation (1200−2000 cm^{-1}).[2a,g,h,3b,l,5a,10b] In contrast, the inverted model **2** in the same aqueous solution (bold dotted lines in Figure 3) showed broadened Qy absorption bands comprised of some components (650−750 nm), indicating that inverted-**2** in the solution afforded several aggregated forms. Three main components were observed from the absorption maxima/shoulder at 660, 684, and 726 nm, which were confirmed from the second-derivative of the original spectrum. On the basis of the reported self-aggregates of zinc methyl 3-acetyl[7c](or 3-formyl[7a])-13^1-*R*-hydroxy-pyropheophorbide-*a*, such species were ascribable to monomeric, dimeric, and oligomeric species of **2** from blue to red. The intense 684 nm peak corresponding to the dimeric species showed that **2** in the aqueous solution hardly formed large oligomers, characteristic of chlorosomal self-aggregates. The CD spectrum of **2** in the solution was complex and mainly ascribable to the two latter species. Fluorescence emission spectra of **1** and **2** in the aqueous media were different, similar to their UV−vis spectra: that of **1** had a fluorescence peak at 730 nm which was typical of chlorosomal self-aggregates in natural BChls and synthetic models, while that of **2** showed an intense emission band at 666 nm, probably due to its residual monomers (see thin solid/broken lines of Figure S1 for **1**/**2** in Supporting Information).

Normal-**1** has the 17-propionate group closer to 13-CHO than 3^1-OH, while the 17-$CH_2CH_2CO_2CH_3$ of inverted-**2** is closer to 13^1-OH. Generally the C=O moiety of the 17-propionate

(13) (a) Tamiaki, H.; Kouraba, M. *Tetrahedron* **1997**, *53*, 10677−10688. (b) Laha, J. K.; Muthiah, C.; Taniguchi, M.; McDowell, B. E.; Ptaszek, M.; Lindsey, J. S. *J. Org. Chem.* **2006**, *71*, 4092−4102.

(14) Oba, T.; Tamiaki, H. *Bioorg. Med. Chem.* **2005**, *13*, 5733−5739.

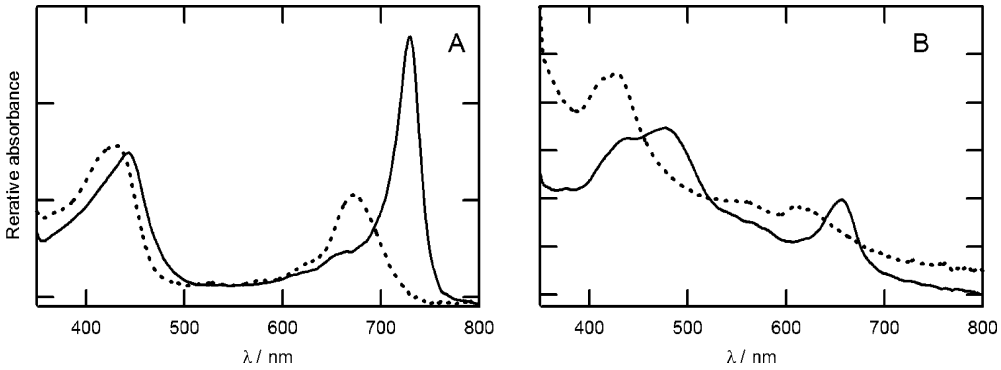

FIGURE 5. UV−vis spectra of zinc chlorins (A, solid/dotted lines for **1**/**2,** respectively) and porphyrins (B, solid/dotted lines for **3**/**4**, respectively) in the solid state.

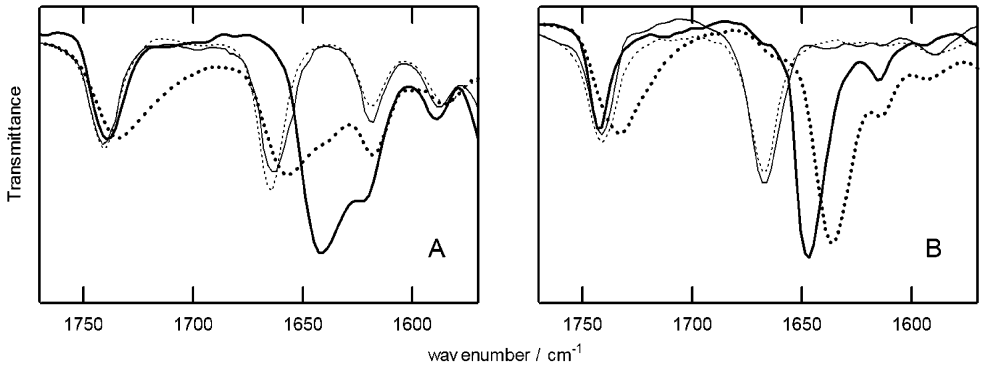

FIGURE 6. FT-IR spectra of zinc chlorins (A, thin and bold solid/dotted lines for **1**/**2** in THF and the solid state, respectively) and porphyrins (B, thin and bold solid/dotted lines for **3**/**4** in THF and the solid state, respectively).

group in chlorosomal chlorins is not involved in the chlorosomal interaction as in the hydrogen-bonding networks,[3a] but the 17-propionate group[15] in **2** would interact with the 13^1-OH intramolecularly. Comparison of the FT-IR spectra of monomeric and oligomeric species is useful for confirming which carbonyl group in a molecule acts as the hydrogen-bonding acceptor in self-aggregates; a vibrational signal of a hydrogen-bonding carbonyl group moves to a lower wavenumber than that of free C═O. A THF and cyclohexane (1:1) solution of **1** or **2** was dropped on glass coated with a thin aluminum film, followed by drying. The UV−vis spectrum of the solid film of **1** (solid line in Figure 5A) showed red-shifted Qy and Soret bands at 729 and 444 nm, respectively, similar to the self-aggregates in the above aqueous micellar solution, indicating that **1** formed chlorosomal *J*-aggregates in the solid film as well as in an aqueous TX-100 solution. The FT-IR spectrum of **1** in the solid state showed three signals in the region from 1600 to 1800 cm^{-1} (bold solid line in Figure 6A), of which the 1621 cm^{-1} peak is assigned to a chlorin skeletal vibration and the 1739 cm^{-1} peak is typical of the free 17^2-C═O signal.[16] The remaining 1641 cm^{-1} peak is thus assigned to the 13-C═O signal. Compared to the spectra of monomeric **1** in neat THF (thin solid line in Figure 6A), the 17^2-C═O showed no shift while the 13-C═O shifted to a lower wavenumber (1664 → 1641 cm^{-1}). Such a spectral change (down-shifted 13-C═O and nonshifted 17^2-C═O) is typical of chlorosomal self-aggregation of natural BChls and synthetic models,[3a] and the presence of 13-C═O···H−O(3^1)···Zn was confirmed in the supramolecules. The UV−vis spectra of the thin film of **2** (broken line in Figure 5A) showed broadened Qy and Soret bands at 672 and 430 nm, respectively, and the Qy band broadened toward a longer wavelength region, probably due to an aggregated species observed in the aqueous solution. The FT-IR spectrum of the solid film of inverted-**2** was complex (bold broken line in Figure 6A), compared to that of its THF solution (thin broken line in Figure 6A). The 3-C═O vibrational peak in the solid film of **2** was situated at 1658 cm^{-1}, close to that in the THF solution (1664 cm^{-1}) with a broadened shoulder (∼1640 cm^{-1}), indicating that the 3-C═O group in the solid film of **2** partially interacted with some other functional groups. It is noteworthy that the 17^2-C═O signal of the solid film of **2** shifted relative to a shorter wavelength region (1734 cm^{-1}) and broadened compared to the 17^2-C═O in the THF solution (1739 cm^{-1}). This means that normal-**1** self-aggregated using the sole 13-C═O moiety as the requisite hydrogen-bonding acceptor while inverted-**2** used both the 3-C═O and the 17^2-C═O in the formation of its self-aggregate. Proposed reasons the inverted-**2** could not form chlorosomal self-aggregates are (i) the hydrogen-bonding ability of the 3-C═O group in **2** is weaker than that of the 13-C═O group in **1** and/or (ii) the 17^2-C═O moiety in **2** disturbs the growth of the self-aggregate to a chlorosomal type.

(15) (a) Abraham, R. J.; Rowan, A. E.; Smith, N. W.; Smith, K. M. *J. Chem. Soc., Perkin Trans. 2* **1993**, 1047−1059. (b) Sato, H.; Uehara, K.; Ishii, T.; Ozaki, Y. *Biochemistry* **1995**, *34*, 7854−7860.

(16) Resonance-Raman (RR) spectra of **1**, **3**, and **4** in the aqueous media supported the assignment of the 17^2-C═O vibrational signals. The region from 1700 to 1800 cm^{-1} in all the RR spectra did not show any signals, indicating that each vibrational signal at around 1730 cm^{-1} in their FT-IR spectra was assigned to the 17^2-C═O vibrational signal because the 17^2-C═O group unconjugated to macrocyclic π-system gave no signal in the RR spectroscopy (see Figure S2 in Supporting Information). The RR spectrum of **2** having less absorbance at the Ar-laser excited wavelength (457.9 nm) was covered by background.

Self-Aggregation of Zinc Porphyrins 3 and 4 (17,18-Dehydrogenated Forms of 1 and 2) in an Aqueous Micellar Solution and the Solid Film. Dehydrogenation of the 17,18-positions in **1**/**2** changed the chlorin π-conjugate systems to porphyrin π-systems of **3**/**4**, in which the electronic environments of the 13- and 3-C═O groups in **3** and **4** became the same (vide supra). In contrast to the same electronic absorption maxima of monomeric **3**/**4**, UV−vis spectra of **3** and **4** in the aqueous solution (solid/dotted lines in Figure 4, Table 1) showed regioisomerically controlled self-aggregation, similar to those of chlorins **1** and **2**. Normal-**3** in the solution gave red-shifted Qy and Soret bands at 647 and 485 nm with the shift values of 1180 and 3020 cm^{-1}, respectively. This spectral change was comparable to that of previously reported self-aggregative porphyrins.[3f,j] On the other hand, inverted-**4** in the solution showed less red-shifted Qy and Soret bands at 631 and 427 nm with residual monomeric species. A difference in the fluorescence emission spectra of **3** and **4** was similar to that between zinc chlorins **1** and **2**: a main emission band of **3** at 660 nm arose from the oligomeric species, while that of **4** at around 600 nm arose from mainly monomers and the others (bold solid/dotted lines for **3**/**4**, Figure S1 in Supporting Information). These results indicated that the regioisomeric control in self-aggregation by the 3,13-inversion was observed not only in chlorins **1**/**2** and but also in porphyrins **3**/**4** and was ascribable to the different situations of the peripheral substituent groups, especially the 17^2-C═O moiety (not to the inherent electronic abilities of their formyl groups).

FT-IR spectral analyses for porphyrins **3** and **4** were also examined. The UV−vis spectrum of the thin film of **3** (solid line in Figure 5B) had red-shifted Qy and Soret bands at 657 and 478 nm, indicating that normal-**3** in the solid state self-aggregated similarly to that in the aqueous TX-100 solution. The thin film of normal-**3** showed its 13-C═O vibration at 1647 cm^{-1} (solid line in Figure 6B), which was down-shifted by 21 cm^{-1} from that in its THF solution (1668 cm^{-1}, thin solid line in Figure 6B). The 17^2-C═O vibrational signal in the solid film of **3** did not show any shift (1741 cm^{-1}). These results are proof that **3** formed chlorosomal self-aggregates using the 13-C═O moiety as a hydrogen-bonding acceptor. The UV−vis spectrum of the thin film of **4** (dotted line in Figure 5B) showed broadened Qy and Soret bands at 609/624 (estimated from the second derivative of the original spectrum) and 430 nm, which were similar to those of **4** in aqueous TX-100 solution. The FT-IR spectrum of the thin film of inverted-**4** (dotted line in Figure 6B) showed a complete downshift in the 3-C═O signal at 1639 cm^{-1}, compared to that in THF (1668 cm^{-1}, thin dotted line in Figure 6B), which was different from the case of the inverted-chlorin **2** showing residual monomeric 3-C═O vibration. This situation can be explained as follows: the stacking ability of the porphyrin chromophore is generally higher than that of chlorin because the π-system in a porphyrin is more level than that in a chlorin and the 3-C═O group interacted with other groups in amorphous self-aggregates of the solid film with less red-shifted bands. Compared to **4** in THF, the 17^2-C═O in the solid film of **4** showed a down-shift (1741 → 1733 cm^{-1}) and a broadening as observed in inverted-chlorin **2**; the 17^2-C═O moiety in the solid film of **4** interacted intra- or intermolecularly with other functional groups to disturb the well-ordered self-aggregation as in chlorosomes. The 13- and 3-C═O groups in **3** and **4** have the same hydrogen-bonding ability due to their symmetrical porphyrin π-systems, which is distinguished from those in **1**/**2**. This explanation is supported by our recent observation that zinc 3-hydroxymethyl-13-formyl-2,7,8,12,17,18-hexaethylporphyrin (lacking the 17^2-ester function) easily formed chlorosomal self-aggregates.[3f]

Contribution of the 17-Propionate Group on Self-Aggregation of Normal-1/3 and Inverted-2/4. As described above, zinc chlorin/porphyrin **1**/**3** possessing 3^1-OH and 13-CHO self-aggregated as did natural chlorosomal BChls, whereas the 17^2-C═O moieties of their 3,13-inverted **2**/**4** disturbed such self-aggregation. Self-aggregative **1**/**3** have the 17^2-C═O groups closer to the 13-CHO while less self-aggregative **2**/**4** have them closer to the 13^1-OH, and the latter 17^2-C═O groups have a potential to form intramolecular hydrogen bonds of 17^2-C═O with 13^1-OH. To clarify why chlorosomal self-aggregation of **2**/**4** was suppressed and what role the 17^2-C═O moiety of **2**/**4** plays in the formed supramolecules, we examined molecular modeling calculations of dimers connected by coordination bonding of 13^1-OH to Zn, which is a basic component of the larger oligomer. Two dimer models have been proposed as the core part of chlorosomal self-aggregation; one is the "opened" dimer[3b,17] in which only a hydroxy group of one molecule coordinates to a zinc atom of another molecule, and the other is the "closed" dimer[18] in which coordination-bonding between a hydroxy group and a zinc atom is mutually formed. Several locally energy-minimized molecular structures were obtained for the two proposed dimers for normal-**1** and inverted-**2** by MM+/PM3 calculations.[3b,6b,7c] The most stable structures of the opened and closed dimers **1** and **2** are shown in Figure 7. In the optimized molecular structures of both the dimers of **1** (far left and left drawings in Figure 7), the 17-propionate group of one molecule (red) is far from the chlorin π-macrocycle of the other and not close to any OH groups (red). In contrast, the 17-propionate groups (red) in dimers of **2** (right and far right drawings in Figure 7) are directed toward the other π-plane and situated at around the 13^1-OH groups (red) coordinating to the zinc atom of the other molecule, as indicated by the black circles and arrows. When an intramolecular atomic distance between the oxygen atoms of the 17^2-C═O and the 13^1-OH groups was restricted to 3.5 Å followed by their energy minimization, the fairly strong hydrogen-bonding between 17^2-C═O and 13^1-OH (angles of the O−H···O were about 147 and 138° for the opened and closed dimer, respectively) was reserved in the dimer without any interference; the total energies of the **2** dimers with/without the restriction were 99.7/98.4 and 124.5/120.6 kcal/mol for the opened and closed dimers, respectively. The energy differences were so small that such a hydrogen bond would contribute to the formation of dimeric **2**. The flexibility of the 17-propionate group in the present zinc complexes is higher than that in the natural BChls and synthetic models due to less steric hindrance around the 15-position because of the lack of the E-ring, so that the 17^2-C═O moiety in **2** could interact with its own 13^1-OH within the core-dimer to disturb the growth and development of larger oligomers. Molecular modeling calculations for zinc porphyrins **3** and **4** also gave similar results, and 17,18-dehydrogenation in **4** caused easier intramolecular access of the 17-propionate to the 13^1-OH group in a dimer than did chlorin **2** possessing the sp^3 carbon atom at the 17-position. From FT-IR experiments of self-aggregated **2**/**4**, however, their 3-C═O groups also acted as hydrogen-bonding

(17) Holzwarth, A. R.; Schaffner, K. *Photosynth. Res.* **1994**, *41*, 225−233.

(18) Wang, Z.-Y.; Umetsu, M.; Kobayashi, M.; Nozawa, T. *J. Am. Chem. Soc.* **1999**, *121*, 9363−9369.

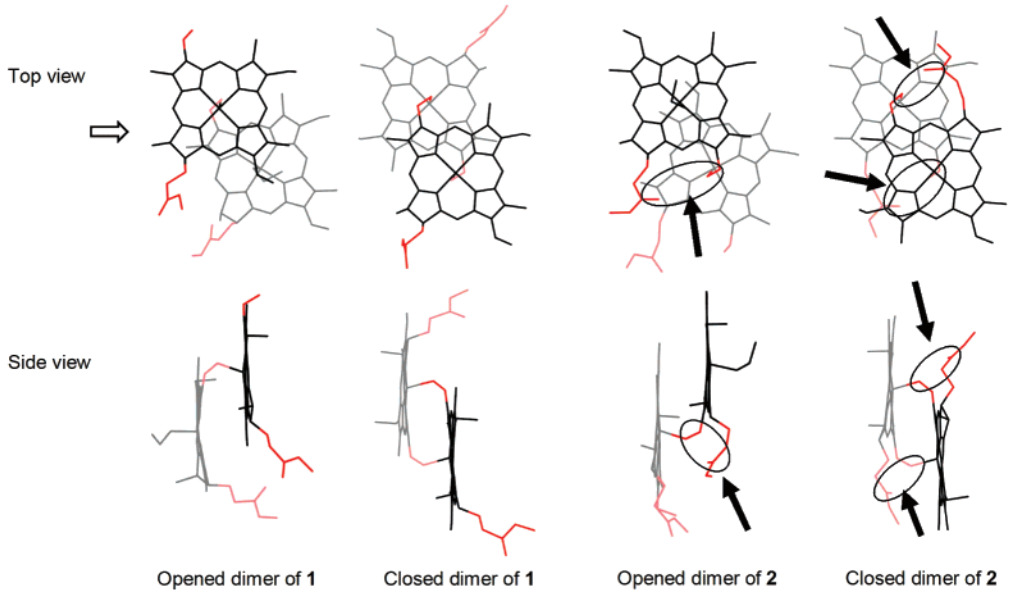

FIGURE 7. Energetically minimized molecular structures of the dimers of **1** and **2**, where the CH_2OH and the 17-$CH_2CH_2CO_2CH_3$ moieties are colored in red. Side views were drawn from a white arrow in the upper figures. Four black arrows and circles in the opened and closed dimers of **2** indicate accessibility of the 13-CH_2OH with the 17-$CH_2CH_2CO_2CH_3$. For opened dimers, the zinc atom of one chlorin was coordinated with an ethanol molecule. The two chlorins in a dimer are distinguished by one chlorin being dark and the other chlorin being light.

acceptors, and the desired hydrogen-bonding of 13^1-OH···O═C-3 was not completely suppressed by the presence of the 17-propionate groups, indicating that the hydrogen-bonding ability of the ester 17^2-C═O moiety is weaker than that of the keto 3-C═O group but enough to disorder the molecular package in the supramolecules of **2**/**4**.

The 17-propionate group in chlorosomal BChls plays a role in stabilizing their supramolecules by the hydrophobic interactions among the long hydrocarbon chain esterified at the 17^2-position and between the esterified chain and the long hydrocarbon of lipid at the chlorosomal surface.[9] No 17^2-C═O moiety is strongly suppressed from involvement in the hydrogen-bonding networks in the main driving force for chlorosomal self-aggregation except in one report:[15b] hydrogen-bonding of the 17^2-C═O with the 3^1-OH in BChl-*c* self-aggregated in a water-saturated CCl_4 solution from a resonance-Raman spectral analysis. The present models **2**/**4** clearly showed that the 3,13-inversion made the intramolecular interaction of the 17^2-ester-C═O with the flexible 13^1-OH possible. The situation of the peripheral substituents other than the OH and C═O groups on a Qy axis is a secondary requisite for chlorosomal self-aggregation and is important in making *J*-aggregates as in chlorosomes.

Conclusion

Zinc 3-hydroxymethyl-13-formyl-chlorin, **1**, and its 3,13-inverted regioisomer, **2**, and their 17,18-dehydrogenated porphyrins, **3** and **4**, were synthesized as chlorosomal chlorophyll models. The 3,13-inversion in zinc chlorins changed the electronic absorption properties in their monomeric states; 3-CHO-13^1-OH-**2** had more red-shifted absorption bands than did 3^1-OH-13-CHO-**1** (a substituent effect on an asymmetric chlorin π-system). Furthermore, in an aqueous TX-100 solution, zinc chlorins **1** and **2** showed different self-aggregation behaviors; **1** self-aggregated to form large oligomers as in natural chlorosomal BChls, while **2** primarily dimerized. 17,18-Dehydrogenation of chlorins **1** and **2** to porphyrins **3** and **4** did not change the self-aggregation behaviors; **3** readily self-aggregated, while **4** aggregated less. The inversion of the 3,13-substituents in the present zinc chlorins and porphyrins strongly affected supramolecular structures of their self-aggregates, and intramolecular interaction of the 17^2-C═O moiety with their 13^1-OH group in **2**/**4** disturbed self-aggregation further. These results indicated that the peripheral substituents in natural BChls (2-, 7-, 8-, 12-, 17-, and 18-positions) have evolved, except for interactive 3^1-OH and 13-C═O on the Qy axis, so that the present 3,13-inverted pigments **2** and **4** rarely form chlorosomal self-aggregates.

Experimental Section

Noncommercial Compound. Rhodochlorin XV dimethyl ester (**5**) was prepared from naturally occurring Chl-*a* according to the previous report.[11]

Synthesis of 13^1,17^3-Dihydroxy-chlorin 6. To a THF solution (50 mL) of **5** (145.0 mg), LAH (160 mg) suspended with THF (10 mL) was added and stirred for 30 min under nitrogen. The reaction mixture was diluted with chloroform and washed with aq 10 % HCl and water, dried over Na_2SO_4, and evaporated to dryness. The residue was purified with FCC (2% methanol/chloroform) and recrystallized from chloroform/hexane to give pure **6** as a green solid (120.2 mg, 92%); mp 212−214 °C; $\lambda_{max}(CH_2Cl_2)$/nm 657 (rel, 0.36), 602 (0.06), 523 (0.02), 498 (0.13), and 406 (1.00); δ_H(600 MHz; $CDCl_3$) 9.83 (1H, s, 5-H), 9.70 (1H, s, 10-H), 9.02 (1H, s, 15-H), 8.87 (1H, s, 20-H), 8.18 (1H, dd, *J* 18, 11, 3-CH), 6.35 (1H, dd, *J* 18, 1, 3^1-CH trans to 3-CH), 6.15 (1H, dd, *J* 11, 1, 3^1-CH cis to 3-CH), 5.92 (2H, s, 13-CH_2), 4.59 (1H, m, 18-H), 4.48 (1H, m, 17-H), 3.84 (2H, q, *J* 8, 8-CH_2), 3.62 (2H, t, *J* 7, 17^2-CH_2), 3.59 (3H, s, 12-CH_3), 3.53 (3H, s, 2-CH_3), 3.38 (3H, s, 7-CH_3), 2.45−2.52, 2.16−2.23 (each 1H, m, 17-CH_2), 1.90 (3H, d, *J* 8 , 18-CH_3), 1.84−1.92, 1.59−1.67 (each 1H, m, 17^1-CH_2), 1.74 (3 H, t, *J* 8, 8^1-CH_3), −2.30 (2H, br s, NH × 2); HRMS (FAB) *m*/*z* 510.3012 (M^+), calcd for $C_{32}H_{38}N_4O_2$ 510.2995.

Synthesis of 13,17^2-Diformyl-chlorin 7. Diol **6** (120.2 mg) was dissolved in dry dichloromethane (50 mL), to which *N*-methyl-

morpholine *N*-oxide (53.0 mg) was added. The mixture was stirred for 5 min, and *n*-Pr_4NRuO_4 (56.8 mg) was added and stirred for 30 min under nitrogen. The reaction mixture was passed through a short silica gel column to separate **7** (3% diethyl ether/dichloromethane). After evaporation in vacuo, the residue was recrystallized from dichloromethane/hexane to give pure **7** as a green solid (52.0 mg, 44%); mp 158−160 °C; $\lambda_{max}(CH_2Cl_2)$/nm 673 (rel, 0.51), 616 (0.11), 536 (0.14), 501 (0.18), and 409 (1.00); δ_H(600 MHz; $CDCl_3$) 11.42 (1H, s, 13-CHO), 9.73 (1H, s, 17^2-CHO), 9.68 (1H, s, 10-H), 9.59 (1H, s, 15-H), 9.55 (1H, s, 5-H), 8.67 (1H, s, 20-H), 8.04 (1H, dd, *J* 18, 11, 3-CH), 6.33 (1H, dd, *J* 18, 1, 3^1-CH trans to 3-CH), 6.17 (1H, dd, *J* 11, 1, 3^1-CH cis to 3-CH), 4.41−4.49 (2H, m, 17-, 18-H), 3.83 (3H, s, 12-CH_3), 3.76 (2H, q, *J* 8, 8-CH_2), 3.44 (3H, s, 2-CH_3), 3.29 (3H, s, 7-CH_3), 2.63−2.75, 2.38−2.53 (each 2H, m, 17-CH_2CH_2), 1.87 (3H, d, *J* 8, 18-CH_3), 1.71 (3H, t, *J* 8, 8^1-CH_3), −1.28 (2H, br s, NH × 2); HRMS (FAB) *m*/*z* 506.2698 (M^+), calcd for $C_{32}H_{34}N_4O_2$ 506.2682.

Synthesis of 13-Formyl-17^2-methoxycarbonyl-chlorin 8. Chlorin **7** (52.0 mg) was dissolved in THF (16 mL) and 2-methyl-2-butene (5 mL), to which an aqueous solution (1 mL) of $HOSO_2NH_2$ (38.0 mg) and an aqueous solution (1 mL) of $NaClO_2$ (29.8 mg) were added. The reaction mixture was stirred for 15 min under nitrogen, poured into water, extracted with dichloromethane, washed with water three times, dried over Na_2SO_4, and evaporated to dryness. The residue was dissolved in THF and treated by an ethereal diazomethane solution. After evaporation in vacuo, the residue was purified on FCC (4% diethyl ether/dichloromethane). Recrystallization from dichloromethane/hexane gave pure **8** as a dark green solid (37.0 mg, 67%); mp 182−184 °C; $\lambda_{max}(CH_2Cl_2)$/nm 673 (rel, 0.51), 616 (0.11), 536 (0.14), 501 (0.18), and 409 (1.00); δ_H(600 MHz; $CDCl_3$) 11.40 (1H, s, 13-CHO), 9.59 (1H, s, 10-H), 9.55 (1H, s, 15-H), 9.48 (1H, s, 5-H), 8.65 (1H, s, 20-H), 7.99 (1H, dd, *J* 18, 11, 3-CH), 6.29 (1H, dd, *J* 18, 1, 3^1-CH trans to 3-CH), 6.13 (1H, dd, *J* 11, 1, 3^1-CH cis to 3-CH), 4.41−4.50 (2H, m, 17-, 18-H), 3.76 (3H, s, 12-CH_3), 3.70 (2H, q, *J* 8, 8-CH_2), 3.64 (3H, s, 17^2-CO_2CH_3), 3.41 (3H, s, 2-CH_3), 3.24 (3H, s, 7-CH_3), 2.69−2.77, 2.56−2.63, 2.35−2.48 (1H + 1H + 2H, m, 17-CH_2-CH_2), 1.87 (3H, d, *J* 8, 18-CH_3), 1.68 (3H, t, *J* 8, 8^1-CH_3), −1.32 (2H, br s, NH × 2); HRMS (FAB) *m*/*z* 536.2792 (M^+), calcd for $C_{33}H_{36}N_4O_3$ 536.2787.

Synthesis of 3,13-Diformyl-chlorin 9. To a THF−1,4-dioxane (4:1, 30 mL) solution of **8** (37.0 mg), a catalytic amount of OsO_4 (approximately 4 mg) was added and stirred for 5 min. Then aq $NaIO_4$ (42.0 mg in 3 mL) was added dropwise and stirred for 4 h under nitrogen. The reaction mixture was poured into water, extracted with dichloromethane, washed with aq 10% NaOAc and water, dried over Na_2SO_4, and evaporated to dryness. The residue was purified on FCC (4% diethyl ether/dichloromethane) and recrystallized from dichloromethane/hexane to give **9** as a brown solid (24.5 mg, 66%); mp 211−213 °C; $\lambda_{max}(CH_2Cl_2)$/nm 701 (rel, 0.78), 642 (0.06), 550 (0.13), 513 (0.10), and 416 (1.00); δ_H(600 MHz; $CDCl_3$) 11.56 (1H, s, 3-CHO), 11.47 (1H, s, 13-CHO), 10.37 (1H, s, 5-H), 9.74 (1H, s, 10-H), 9.73 (1H, s, 15-H), 8.91 (1H, s, 20-H), 4.49−4.57 (2H, m, 17-, 18-H), 3.88 (3H, s, 12-CH_3), 3.79 (2H, q, *J* 8, 8-CH_2), 3.78 (3H, s, 2-CH_3), 3.65 (3H, s, 17^2-CO_2-CH_3), 3.36 (3H, s, 7-CH_3), 2.73−2.81, 2.59−2.66, 2.37−2.50 (1H + 1H + 2H, m, 17-CH_2CH_2), 1.90 (3H, d, *J* 8, 18-CH_3), 1.74 (3H, t, *J* 8, 8^1-CH_3), −1.58 (2H, s, NH × 2); HRMS (FAB) *m*/*z* 538.2584 (M^+), calcd for $C_{32}H_{34}N_4O_4$ 538.2580.

Synthesis of Zinc 3,13-Diformyl-chlorin 10. To a dichloromethane (20 mL) solution of **9** (24.5 mg), methanol saturated with $Zn(OAc)_2 \cdot 2H_2O$ was added and stirred for 2 h under nitrogen. The reaction mixture was poured into water, extracted with dichloromethane, washed with aq 4% $NaHCO_3$ and water, dried over Na_2SO_4, and evaporated to dryness. The residue was purified on FCC (1% methanol/dichloromethane) and recrystallized from chloroform/hexane to give **10** as a green solid (26.3 mg, 96%); mp > 300 °C; λ_{max}(THF)/nm 676 (rel, 1.21), 628 (0.14), 578 (0.07), 531 (0.03), and 437 (1.00); δ_H(600 MHz; 1 v/v % pyridine-d_5−$CDCl_3$) 11.43 (1H, s, 3-CHO), 11.33 (1H, s, 13-CHO), 10.28 (1H, s, 5-H), 9.63 (1H, s, 10-H), 9.46 (1H, s, 15-H), 8.60 (1H, s, 20-H), 4.39−4.45 (2H, m, 17-, 18-H), 3.80 (2H, q, *J* 8, 8-CH_2), 3.79 (3H, s, 12-CH_3), 3.68 (3H, s, 2-CH_3), 3.61 (3H, s, 17^2-CO_2CH_3), 3.37 (3H, s, 7-CH_3), 2.59−2.67, 2.35−2.43 (each 1H, m, 17-CH_2), 2.47−2.54, 2.17−2.24 (each 1H, m, 17^1-CH_2), 1.77 (3H, d, *J* 8, 18-CH_3), 1.72 (3H, t, *J* 8, 8^1-CH_3); δ_C(150 MHz; 1 v/v % pyridine-d_5−$CDCl_3$) 188.8 ($C3^1$), 188.5 ($C13^1$), 173.7, 165.7, 163.5, 150.0, 149.5, 149.2, 148.9, 146.7, 144.4, 144.3, 143.4, 142.7, 135.9, 133.2, 129.9 (C1, 2, 3, 4, 6, 7, 8, 9, 11, 12, 13, 14, 16, 17^3, 19), 103.9 (C5), 102.9 (C10), 96.6 (C15), 93.8 (C20), 53.8 (C17), 51.6 ($C17^4$), 46.8 (C18), 32.2 ($C17^1$), 30.7 ($C17^2$), 23.6 ($C18^1$), 19.5 ($C8^1$), 17.5 ($C8^2$), 11.7 ($C12^1$), 11.6 ($C2^1$), 11.2 ($C7^1$); HRMS (FAB) *m*/*z* 600.1709 (M^+), calcd for $C_{32}H_{32}N_4O_4{}^{64}Zn$ 600.1715.

Synthesis of Zinc 3-Hydroxymethyl-13-formyl-chlorin 1 and Zinc 3-Formyl-13-hydroxymethyl-chlorin 2. To a dichloromethane (20 mL) solution of **10** (26.3 mg), *t*-$BuNH_2 \cdot BH_3$ (8.5 mg) was added and stirred under nitrogen. The reaction was monitored by TLC and stopped by a complete disappearance of starting material with a concomitant appearance of two new spots (both corresponding to **1**/**2** and **11**). The reaction mixture was poured into water, extracted with dichloromethane, washed with aq 1% $KHSO_4$ and water, dried over Na_2SO_4, and evaporated to dryness. A regioisomeric mixture of monoreduced **1** and **2** and doubly reduced 3^1,13^1-dihydroxy-chlorin-**11** was separated on FCC (1−2 and 3% methanol/dichloromethane for **1**/**2** and **11**, respectively). The regioisomeric mixture of **1** and **2** was separated by RP-HPLC (methanol/water/pyridine = 90/9/1, C18, 10 mm i.d. × 250 mm, 2.0 mL/min); **1** and **2** were eluted at 13 and 15 min, respectively. Each regioisomerically pure **1** and **2** as well as **11** was recrystallized from dichloromethane/hexane to give a pure compound: **1**, 11.0 mg in 42%; **2**, 3.4 mg in 13%; and **11**, 5.0 mg in 19%.

1: mp > 300 °C; λ_{max}(THF)/nm 642 (rel, 0.72), 597 (0.10), 557 (0.04), 514 (0.03), and 418 (1.00); δ_H(600 MHz; 1 v/v % pyridine-d_5−$CDCl_3$) 11.29 (1H, s, 13-CHO), 9.60 (1H, s, 10-H), 9.45 (1H, s, 5-H), 9.33 (1H, s, 15-H), 8.39 (1H, s, 20-H), 5.84 (2H, s, 3-CH_2), 4.31−4.39 (2H, m, 17-, 18-H), 3.78 (2H, q, *J* 8, 8-CH_2), 3.76 (3H, s, 12-CH_3), 3.59 (3H, s, 17^2-CO_2CH_3), 3.33 (3H, s, 2-CH_3), 3.29 (3H, s, 7-CH_3), 2.54−2.63, 2.33−2.41 (each 1H, m, 17-CH_2), 2.43−2.50, 2.13−2.19 (each 1H, m, 17^1-CH_2), 1.74 (3H, d, *J* 8, 18-CH_3), 1.70 (3H, t, *J* 8, 8^1-CH_3); δ_C(150 MHz; 1 v/v % pyridine-d_5−$CDCl_3$) 188.4 ($C13^1$), 173.8, 167.5, 161.9, 153.9, 149.4, 149.2, 146.9, 146.6, 144.4, 142.8, 141.3, 139.7, 136.1, 133.5, 128.7 (C1, 2, 3, 4, 6, 7, 8, 9, 11, 12, 13, 14, 16, 17^3, 19), 104.1 (C10), 99.8 (C5), 95.9 (C15), 92.4 (C20), 56.6 ($C3^1$), 53.2 (C17), 51.6 ($C17^4$), 47.2 (C18), 32.3 ($C17^1$), 30.7 ($C17^2$), 23.4 ($C18^1$), 19.6 ($C8^1$), 17.6 ($C8^2$), 11.8 ($C12^1$), 11.4 ($C2^1$), 11.2 ($C7^1$); HRMS (FAB) *m*/*z* 602.1879 (M^+), calcd for $C_{32}H_{34}N_4O_4{}^{64}Zn$ 602.1872.

2: mp > 300 °C; λ_{max}(THF)/nm 653 (rel, 0.83), 607 (0.11), 563 (0.05), 521 (0.06), 425 (1.00), and 414 (0.99); δ_H(600 MHz; 1 v/v % pyridine-d_5−$CDCl_3$) 11.48 (1 H, s, 3-CHO), 10.36 (1 H, s, 5-H), 9.48 (1 H, s, 10-H), 8.73 (1 H, s, 15-H), 8.66 (1H, s, 20-H), 5.82 (2H, s, 13-CH_2), 4.38−4.47 (2H, m, 17-, 18-H), 3.82 (2H, q, *J* 8, 8-CH_2), 3.71 (3H, s, 2-CH_3), 3.53 (3H, s, 17^2-CO_2CH_3), 3.49 (3H, s, 12-CH_3), 3.40 (3H, s, 7-CH_3), 2.67 (1H, br s, 13^1-OH), 2.58−2.67, 2.47−2.54, 2.38−2.46, 2.13−2.20 (each 1H, m, 17-CH_2CH_2), 1.79 (3H, d, *J* 8, 18-CH_3), 1.72 (3H, t, *J* 8, 8^1-CH_3); δ_C(150 MHz; 1 v/v % pyridine-d_5−$CDCl_3$) 188.9 ($C3^1$), 173.9, 163.4, 162.8, 151.7, 148.0, 147.6, 147.0, 142.4, 141.2, 141.0, 140.2, 136.2, 132.1 (C1, 2, 3, 4, 6, 7, 8, 9, 11, 12, 13, 14, 16, 17^3, 19, two carbon signals which overlapped the others), 104.3 (C10), 99.8 (C10), 93.9 (C20), 93.6 (C15), 56.6 ($C13^1$), 54.2 (C17), 51.6 ($C17^4$), 46.4 (C18), 32.0, 30.7 ($C17^1$, 17^2), 23.8 ($C18^1$), 19.6 ($C8^1$), 17.6 ($C8^2$), 11.7 ($C2^1$), 11.5 ($C12^1$), 11.3 ($C7^1$); HRMS (FAB) *m*/*z* 602.1891 (M^+), calcd for $C_{32}H_{34}N_4O_4{}^{64}Zn$ 602.1872.

Zinc 3^1,13^1-dihydroxy-chlorin **11:** mp > 300 °C; λ_{max}(THF)/nm 618 (rel, 0.31), 574 (0.05), 538 (0.03), 506 (0.03), and 406 (1.00); δ_H(600 MHz; 1 v/v % pyridine-d_5−$CDCl_3$) 9.66 (1H, s, 5-H), 9.59

(1H, s, 10-H), 8.71 (1H, s, 15-H), 8.56 (1H, s, 20-H), 5.92 (2H, s, 3-CH_2), 5.84, 5.82 (each 1H, d, *J* 12, 13-CH_2), 4.43 (1H, m, 18-H), 4.38 (1H, m, 17-H), 3.84 (2H, q, *J* 8, 8-CH_2), 3.51 (3H, s, 12-CH_3), 3.50 (3H, s, 17^2-CO_2CH_3), 3.40 (3H, s, 2-CH_3), 3.37 (3H, s, 7-CH_3), 2.55−2.62, 2.37−2.44 (each 1H, m, 17-CH_2), 2.43−2.49, 2.07−2.12 (each 1H, m, 17^1-CH_2), 1.76 (3H, d, *J* 8, 18-CH_3), 1.72 (3H, t, *J* 8, 8^1-CH_3); δ_C(150 MHz; 1 v/v % pyridine-d_5−$CDCl_3$) 174.0, 164.4, 161.4, 151.2, 150.1, 145.9, 144.6, 144.2, 143.5, 140.8, 139.2, 138.6, 134.1, 134.0, 133.4 (C1, 2, 3, 4, 6, 7, 8, 9, 11, 12, 13, 14, 16, 17^3, 19), 101.2 (C10), 100.7 (C5), 93.0 (C15), 92.3 (C20), 56.7_2 ($C3^1$), 56.6_8 ($C13^1$), 53.7 (C17), 51.5 ($C17^4$), 46.9 (C18), 32.2 ($C17^1$), 30.6 ($C17^2$), 23.7 ($C18^1$), 19.6 ($C8^1$), 17.8 ($C8^2$), 11.5 ($C12^1$), 11.4 ($C2^1$), 11.3 ($C7^1$); HRMS (FAB) *m*/*z* 604.2031 (M^+), calcd for $C_{32}H_{36}N_4O_4{}^{64}Zn$ 604.2028.

Synthesis of Zinc 3-Hydroxymethyl-13-formyl-porphyrin 3. To an acetone solution (10 mL) of **1** (approximately 2 mg), an acetone solution (5 mL) of DDQ (5.0 mg) was carefully added dropwise and stirred. After complete disappearance of the Qy band in **1** (642 nm), the reaction mixture was poured into aq 4% $KHSO_4$ and extracted with dichloromethane, washed with aq 4% $NaHCO_3$ and water, dried over Na_2SO_4, and evaporated to dryness. The residue was purified with FCC (1−2% methanol/dichloromethane) and recrystallized from chloroform/hexane to give pure **3** in a quantitative yield; mp > 300 °C; λ_{max}(THF)/nm 601 (rel, 0.12), 555 (0.05), and 423 (1.00); δ_H(600 MHz; 1 v/v % pyridine-d_5−$CDCl_3$) 11.64 (1H, s, 13-CHO), 10.77 (1H, s, 15-H), 10.12 (2H, s, 5-, 10-H), 9.93 (1H, s, 20-H), 6.10 (2H, s, 3-CH_2), 4.40 (2H, t, *J* 8, 17-CH_2), 4.05 (2H, q, *J* 8, 8-CH_2), 4.01 (3H, s, 12-CH_3), 3.68 (3H, s, 17^2-CO_2CH_3), 3.67 (3H, s, 2-CH_3), 3.60 (3H, s, 18-CH_3), 3.58 (3H, s, 7-CH_3), 3.31 (2H, t, *J* 8, 17^1-CH_2), 1.85 (3H, t, *J* 8, 8^1-CH_3); HRMS (FAB) *m*/*z* 600.1729 (M^+), calcd for $C_{32}H_{32}N_4O_4{}^{64}$-Zn 600.1715.

Synthesis of Zinc 3-Formyl-13-hydroxymethyl-porphyrin 4. Similar to the synthesis of **3** from **1**, DDQ oxidation of chlorin **2** (Qy maxima = 653 nm) gave porphyrin **4** in a quantitative yield; mp > 300 °C; λ_{max}(THF)/nm 601 (rel, 0.12), 555 (0.05), and 423 (1.00); δ_H(600 MHz; 1 v/v % pyridine-d_5−$CDCl_3$) 11.62 (1H, s, 3-CHO), 10.81 (1H, s, 5-H), 10.12 (1H, s, 20-H), 10.09 (1H, s, 15-H), 9.92 (1H, s, 10-H), 6.10 (2H, s, 13-CH_2), 4.39 (2H, t, *J* 8, 17-CH_2), 4.03 (2H, q, *J* 8, 8-CH_2), 3.99 (3H, s, 2-CH_3), 3.68 (3H, s, 12-CH_3), 3.61 (6H, s, 7-, 18-CH_3), 3.49 (3H, s, 17^2-CO_2CH_3), 3.23 (2H, t, *J* 8, 17^1-CH_2), 1.84 (3H, t, *J* 8, 8^1-CH_3); HRMS (FAB) *m*/*z* 600.1721 (M^+), calcd for $C_{32}H_{32}N_4O_4{}^{64}$Zn 600.1715.

Acknowledgment. We thank Dr. Tomohiro Miyatake of Ryukoku University for his helpful assistance in the measurement of the HRMS spectra as well as Dr. Tadashi Mizoguchi and Mr. Shosuke Nakabayashi of Ritsumeikan University for experimental assistance in the measurement of the RR and surface absorption spectra, respectively. This work was partially supported by Grants-in-Aid for Scientific Research (Grant No. 17029065) on Priority Areas (417) from MEXT and for Scientific Research (B) (Grant No. 15350107) from JSPS as well as by the "Academic Frontier" Project for Private Universities: matching fund subsidy from MEXT, 2003−2007.

Supporting Information Available: Fluorescence spectra of **1**−**4** in aqueous TX-100 solution, RR spectra of **1**, **3**, and **4** in aqueous TX-100 solution, 1D/2D ^1H and ^{13}C NMR spectra of **1**−**4**, **10**, and **11**. This material is available free of charge via the Internet at http://pubs.acs.org.

JO0623282